

Fig. S1 Particle number concentrations of different modes between NPF days and non-NPF days.

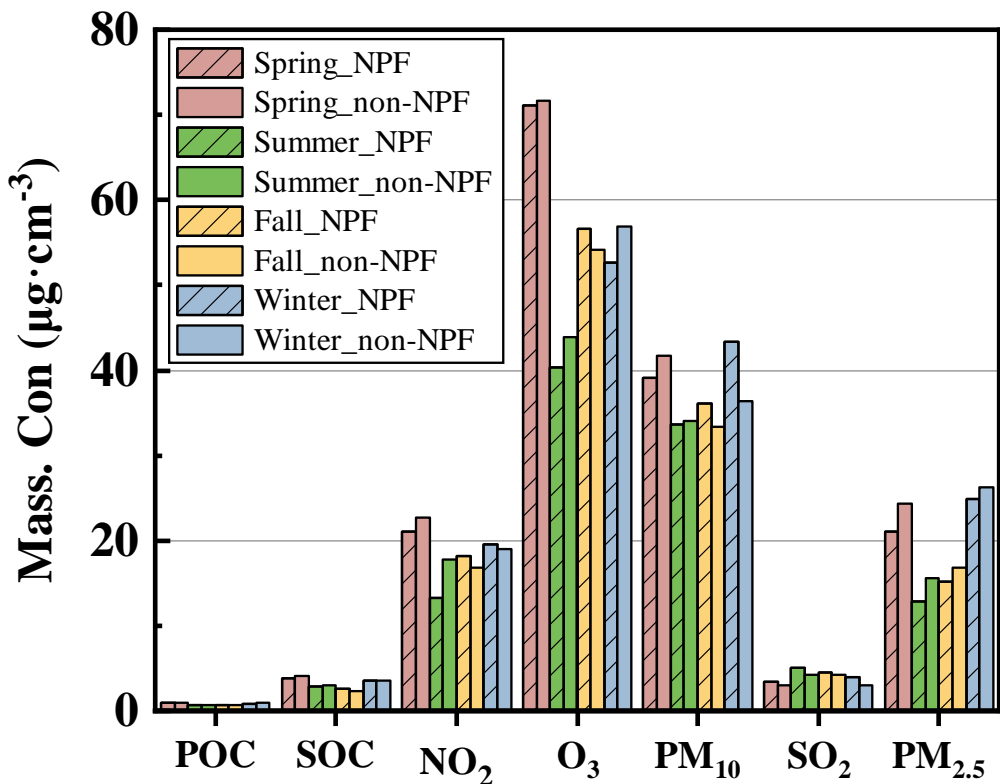


Fig. S2 Mass concentrations of particulate pollutants between NPF days and non-NPF days.

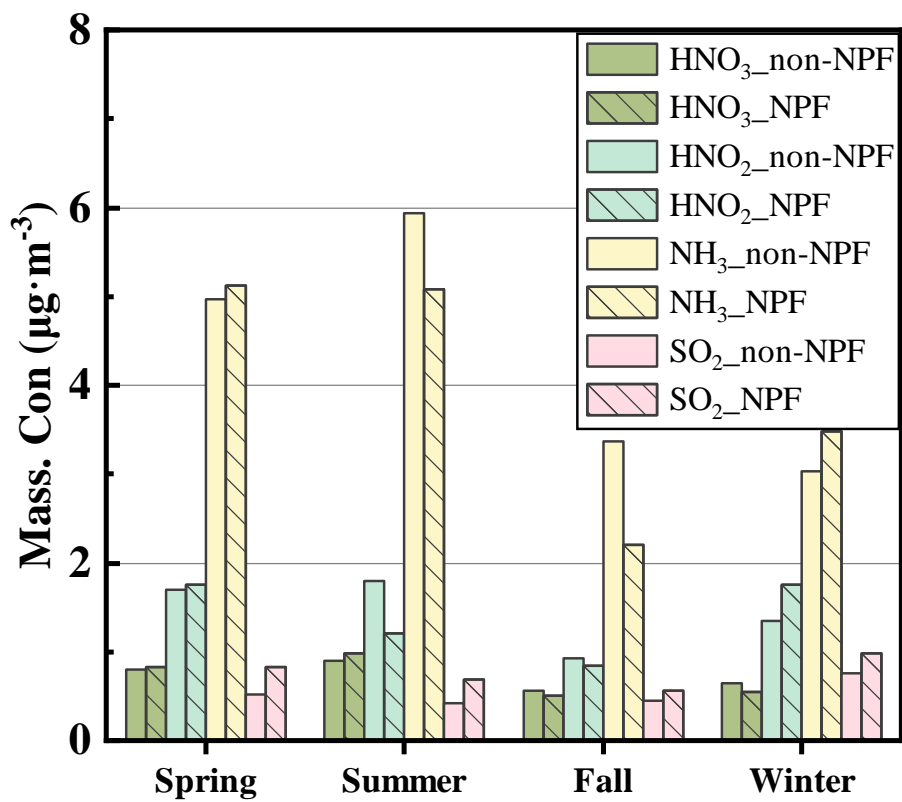


Fig.S3 Mass concentrations of precursor gases (e.g., SO_2 , NO_2 , O_3 , NH_3) between NPF days and non-NPF days.

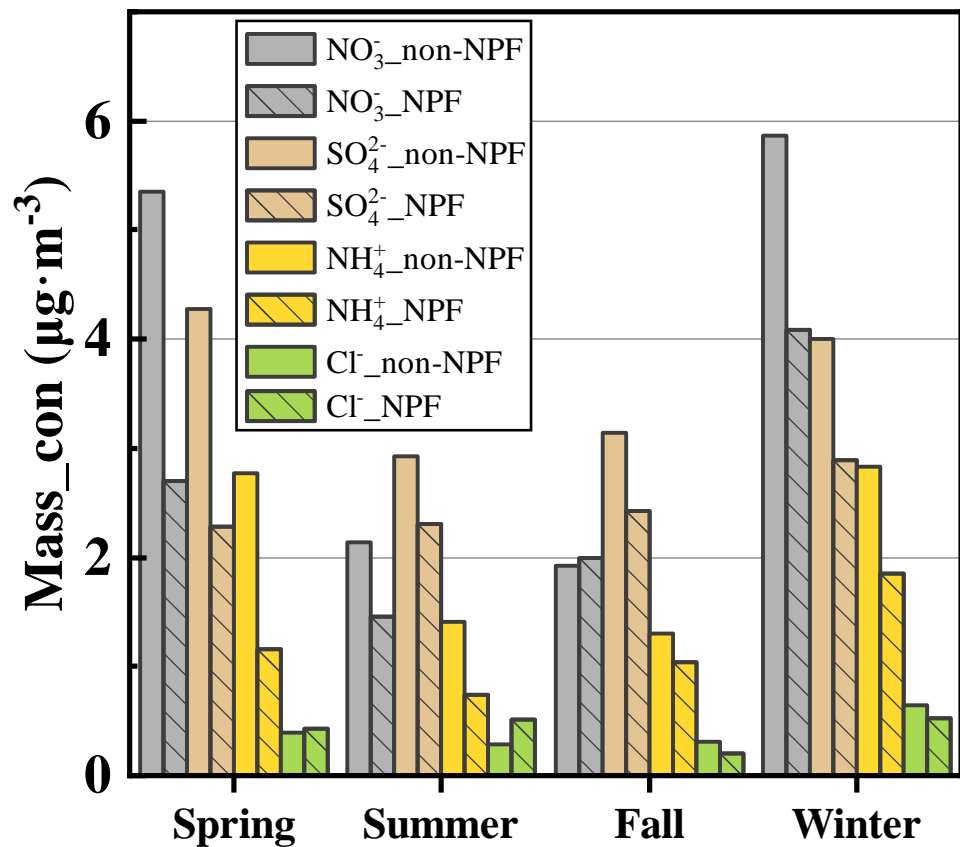


Fig.S4 Mass concentrations of major ions (SO_4^{2-} , NO_3^- , NH_4^+) between NPF days and non-NPF days.

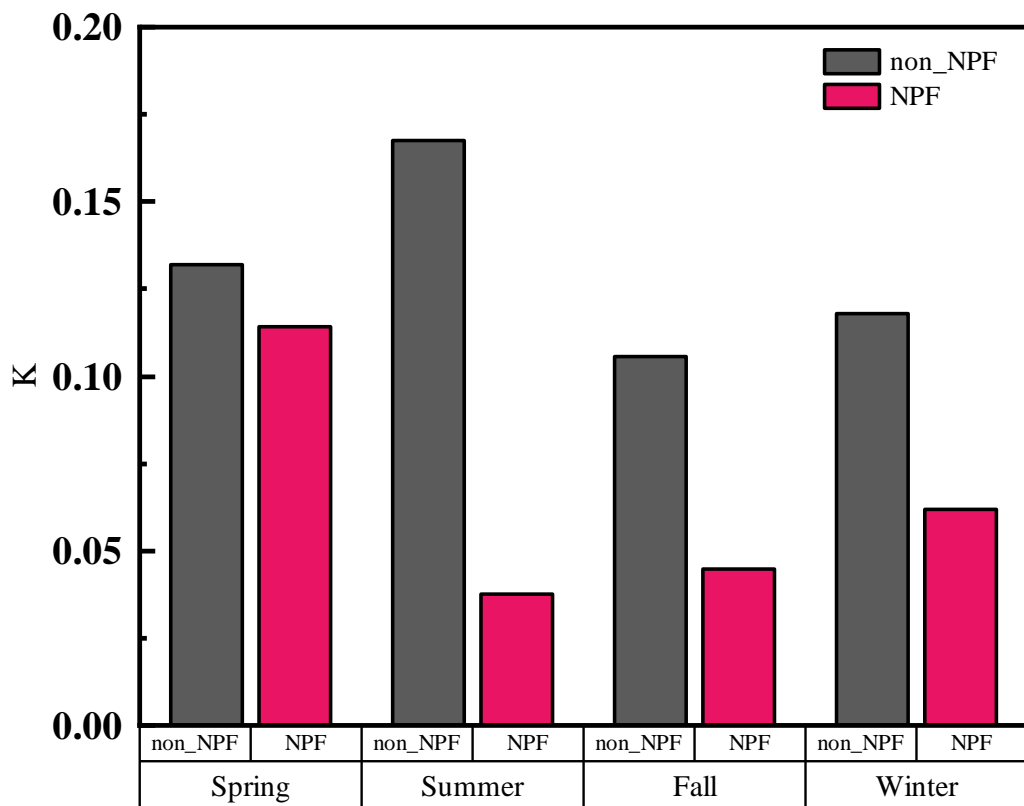


Fig.S5 The mean hygroscopicity parameter (κ) between NPF days and non-NPF days.

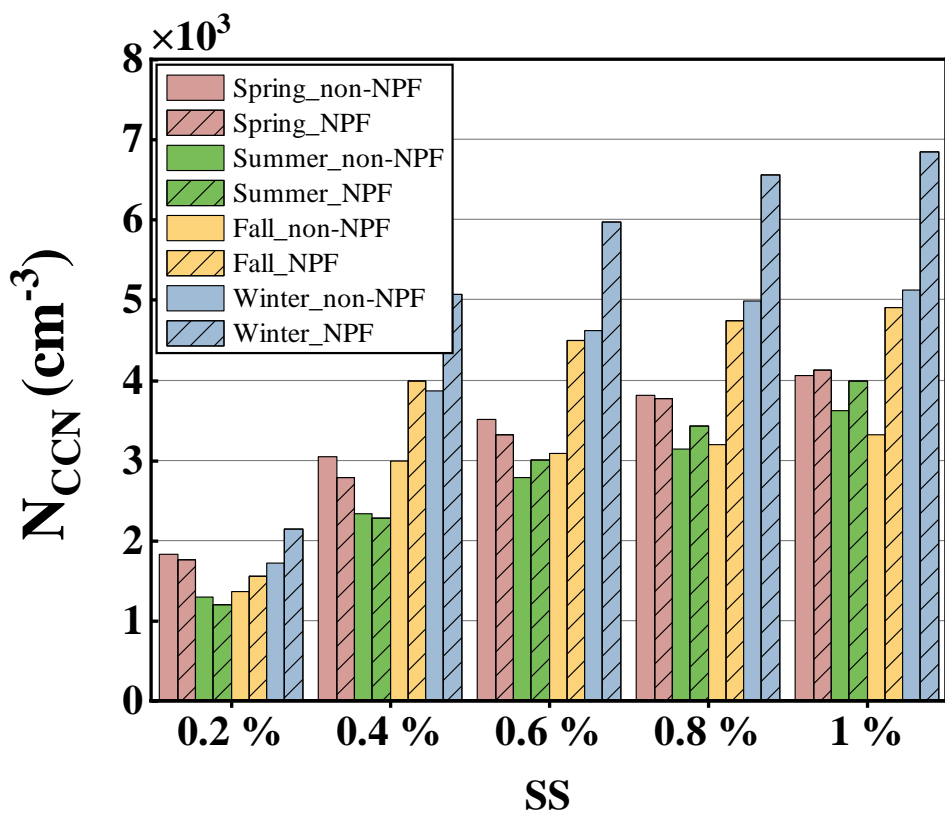


Fig.S6 Cloud condensation nuclei number concentrations (N_{CCN}) at 0.2-1.0% supersaturations between NPF days and non-NPF days.

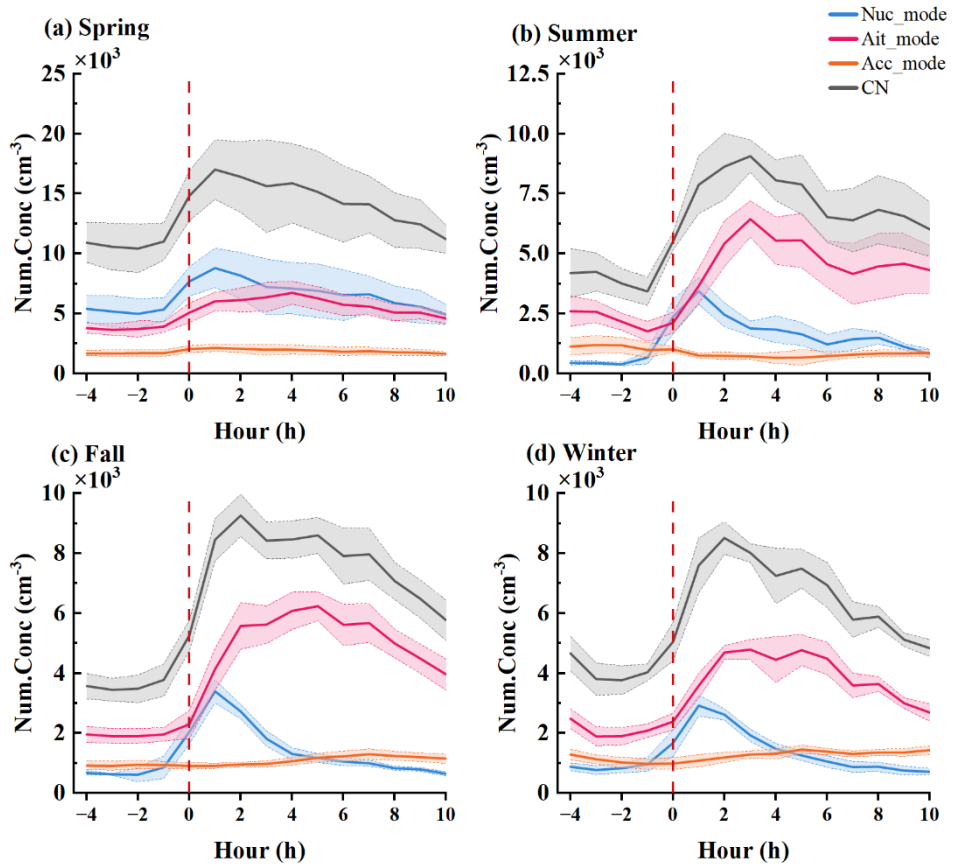


Fig.S7 Temporal evolution of particle number concentrations in the nucleation, Aitken, and accumulation modes during NPF events.

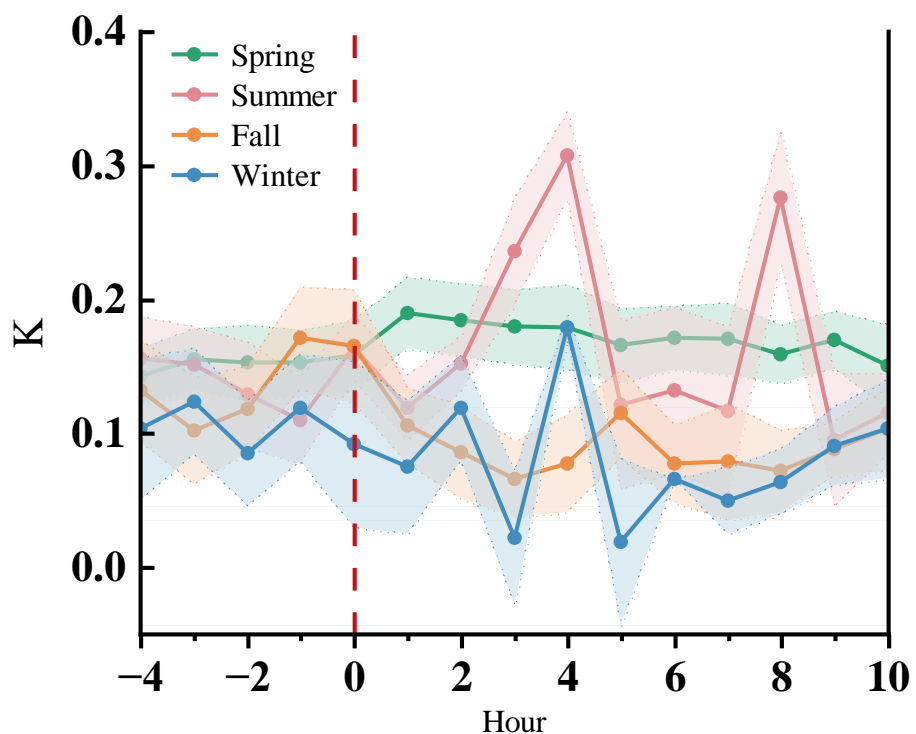


Fig. S8 Temporal evolution of the particle hygroscopicity parameter (κ) during NPF events.

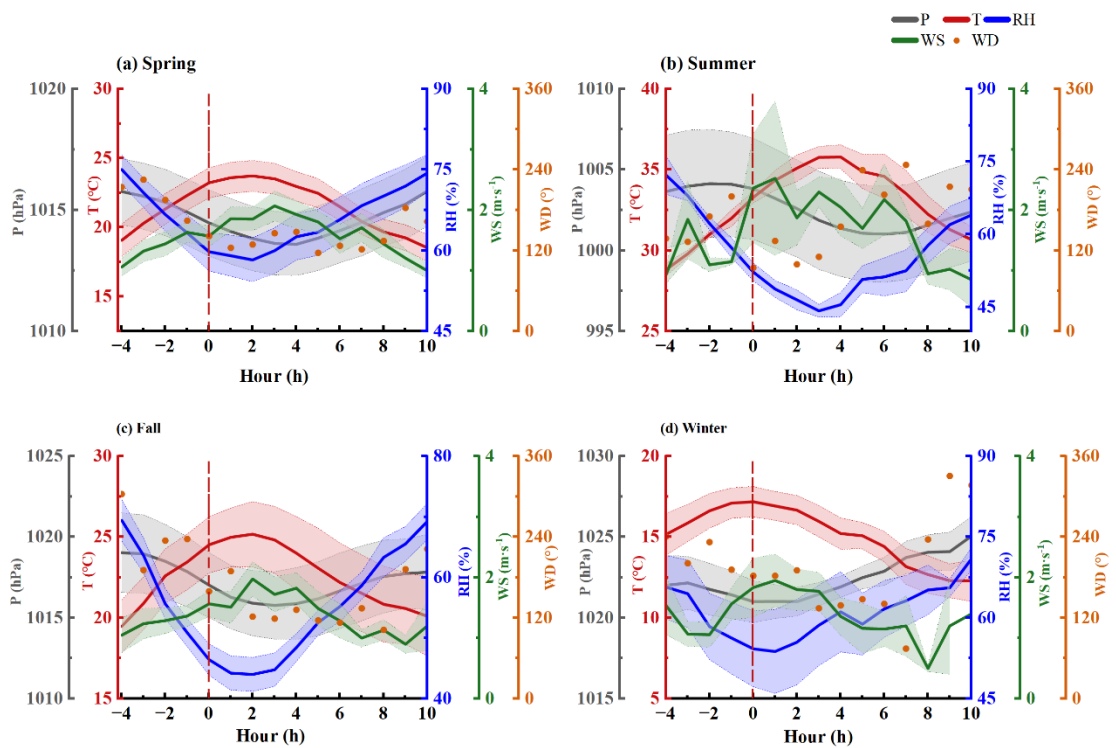


Fig. S9 Evolution of meteorological parameters (Pressure, Temperature, RH, WS, WD) during NPF events.

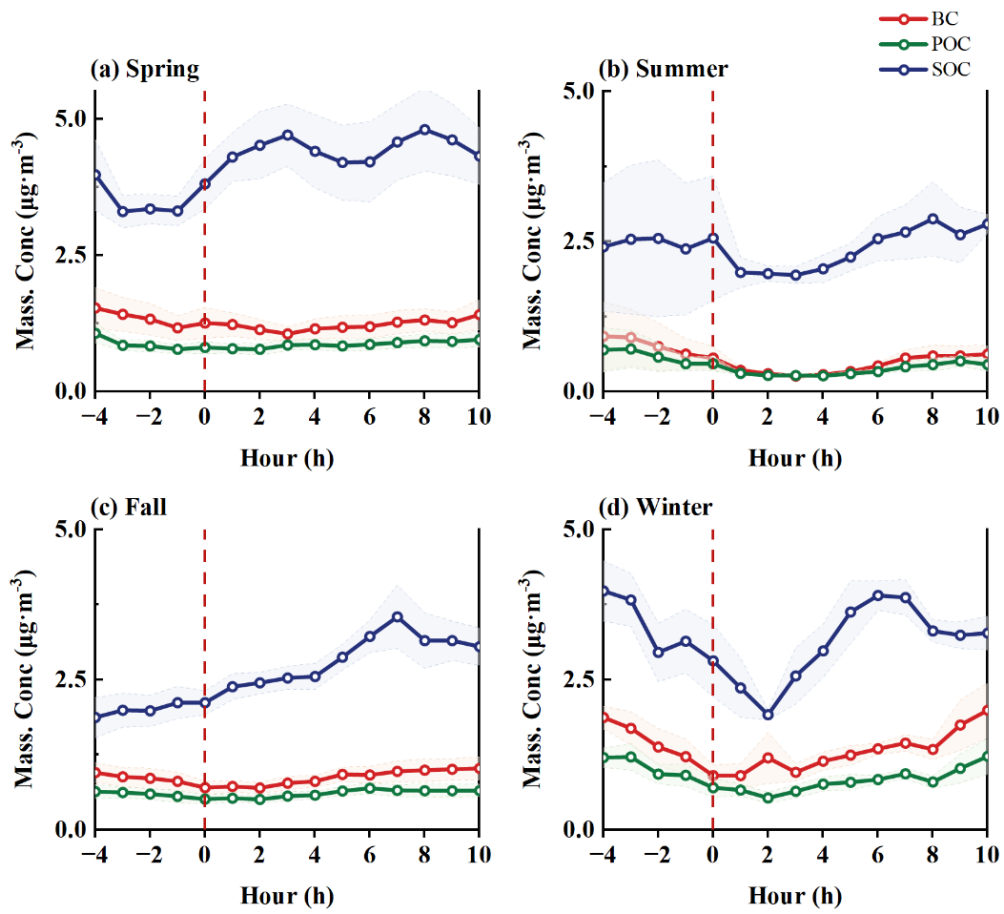


Fig. S10 Temporal variations in the mass concentrations of black carbon (BC), primary organic carbon (POC), and secondary organic carbon (SOC) during NPF events.

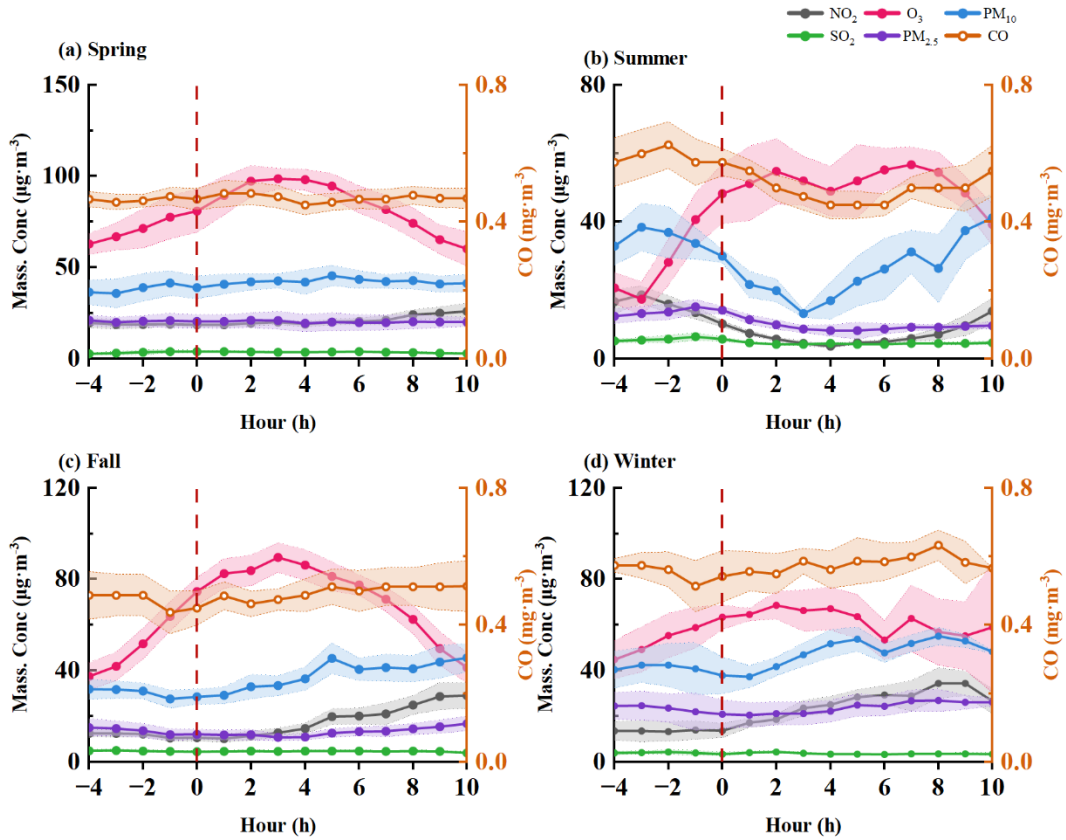


Fig. S11 Evolution of key atmospheric environmental factors during NPF events.

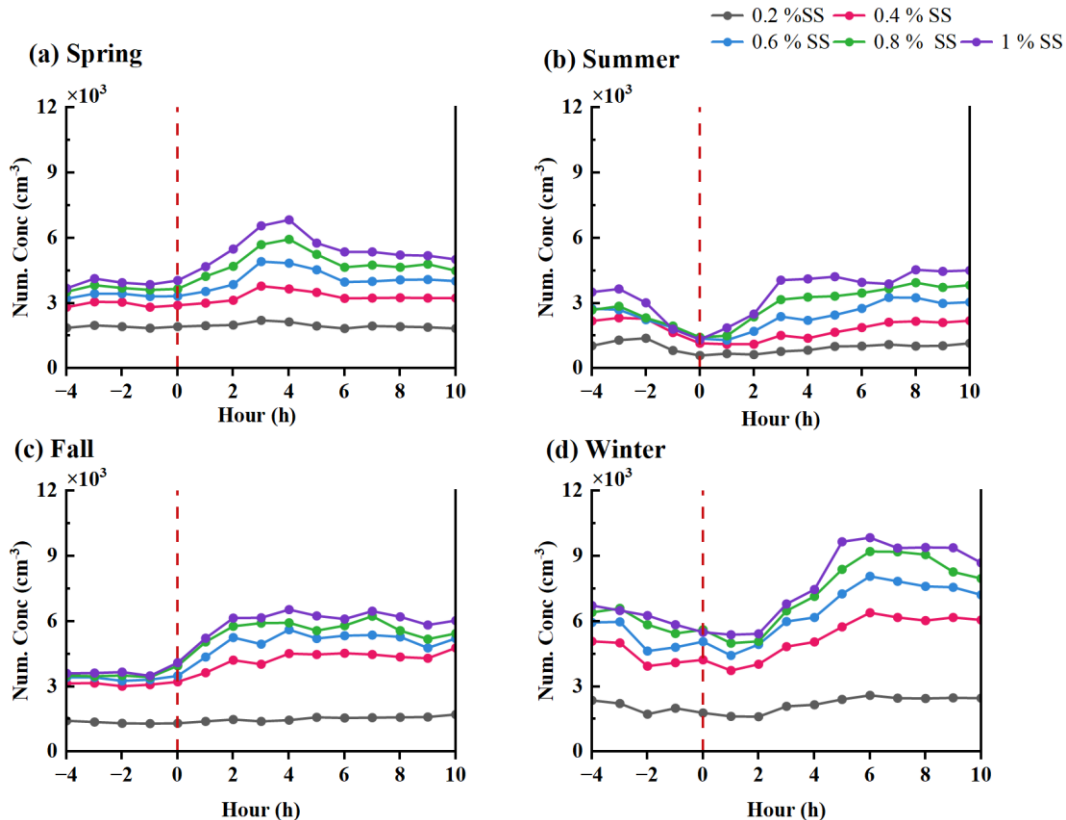


Fig. S12 Temporal evolution of cloud condensation nuclei (CCN) number concentrations at different supersaturations during NPF events.